Endonuclease III Interactions with DNA Substrates. 2. The DNA Repair Enzyme Endonuclease III Binds Differently to Intact DNA and to Apyrimidinic/Apurinic DNA Substrates As Shown by Tryptophan Fluorescence Quenching†

Dongxia Xing,‡ Roswitha Dorr,‡ Richard P. Cunningham,§ and Charles P. Scholes*,‡

Departments of Chemistry and Biological Sciences, University at Albany, State University of New York, Albany, New York 12222

Received July 14, 1994; Revised Manuscript Received November 1, 1994®

ABSTRACT: We have measured the fluorescence of the DNA repair enzyme endonuclease III to discover perturbation to its tryptophans by undamaged DNA and AP (apyrimidinic or apurinic) DNA and to estimate binding affinity for intact and AP DNAs. Endonuclease III has two tryptophans, Trp^{132} in a helix−hairpin−helix region of possible flexibility near the active site for AP lyase activity and Trp^{178} in the domain containing the iron−sulfur center of endonuclease III; Trp^{132} is the more solvent-accessible tryptophan [Kuo, C.-F., McRee, D. E., Fisher, C. L., O'Handley, S. F., & Cunningham, R. P. (1992) *Science 258*, 434−440]. The fluorescence emission peak wavelength near 350 nm (excitation at 290 nm) indicated an exposure of the fluorescing tryptophans to a polar environment. Quenching of tryptophan fluorescence by iodide demonstrated that there are indeed two tryptophans which are differently accessible to anionic quencher. Significant (~60%) fluorescence quenching occurred when endonuclease III was titrated with high molecular weight duplex undamaged poly(dAdT). The apparent second-order nonspecific binding constant to poly(dAdT) was 4×10^7 M^{-1}, and there were approximately 12 base pairs per endonuclease III binding site for binding to poly(dAdT). This nonspecific binding to duplex DNA had ionic character, and there was no fluorescence quenching brought on by single-stranded DNA. A comparison between fluorescence quenching titrations of high molecular weight duplex DNA and undamaged duplex 19-mer oligonucleotide showed that the binding constant to the high molecular weight DNA was ~400-fold larger than to the undamaged 19-mer. Gel shift and footprinting experiments clearly show that duplex oligonucleotide substrates containing a central AP or noncatalyzable reduced AP site strongly bind to endonuclease III [O'Handley, S., Scholes, C. P., & Cunningham, R. P. (1995) *Biochemistry 34*, 2528−2536], but there was reduced fluorescence quenching in the presence of AP or reduced AP oligonucleotide substrates. The specific binding of such AP substrates must involve fluorescing tryptophan(s) differently from nonspecific binding to undamaged duplex DNA. This difference may correlate with the difference between the five- to seven-base pair size of the specific, AP-centered binding site determined by footprinting (companion paper) and the 12-base pair size of the nonspecific binding site determined from these fluorescence measurements. In competition with oligonucleotide 19-mer substrates containing either a central AP site or a reduced AP site, tryptophan fluorescence quenching brought on by high molecular weight poly(dAdT) DNA was eliminated and reduced to nearly its unquenched value. Quantitation of this competitive elimination indicated a specific binding constant of order 4×10^7 M^{-1} for the reduced AP 19-mer substrate and a binding constant much greater than 10^8 M^{-1} for the AP 19-mer substrate.

Endonuclease III (endo III)[1] from *Escherichia coli* is a DNA repair enzyme that has both DNA *N*-glycosylase and apurinic/apyrimidinic (AP) lyase activities (Katcher & Wallace, 1983; Doetsch & Cunningham, 1990). As an AP lyase, the enzyme introduces a single-strand break at the AP site where loss of a base has occurred. Bacteria, yeast, bovine, and human cells share a conserved class of enzymes with similar molecular weights and the same substrate specificity as endo III from *E. coli* for damaged DNA cleavage (Doetsch et al., 1987). The overall purpose of this and the companion paper is to characterize the general binding of endo III with DNA and the specific recognition by endo III of an AP site. In this paper we use the quenching of the intrinsic tryptophan fluorescence of endo III to spectroscopically characterize the binding of endo III and to infer binding constants with intact DNA and specifically AP-damaged substrate. In the ac-

† This work was supported in part by grants from the NIH (GM 35103 to C.P.S.) and the NSF (DMB8917741 to R.P.C.).

* To whom correspondence should be addressed.

‡ Department of Chemistry.

§ Department of Biological Sciences.

® Abstract published in *Advance ACS Abstracts,* February 1, 1995.

[1] Abbreviations: endo III, endonuclease III; poly(dAdT), duplex poly(dA-dT)−poly(dA-dT); AP, apyrimidinic/apurinic site; rAP, reduced apyrimidinic site; (U•A)-19-mer, d(GCAGCGCAG(U)CAGCCGACG)•d(CGTCGGCTGACTGCGCTGC); (AP•A)-19-mer, d(GCAGCGCAG(AP)CAGCCGACG)•d(CGTCGGCTGACTGCGCTGC); (rAP•A)-19-mer, d(GCAGCGCAG(rAP)CAGCCGACG)•d(CGTCGGCTGACTGCGCTGC). (U•A)-39-mer and (rAP•A)-39-mer are described in the accompanying paper (O'Handley et al., 1995). HM-K_{obs}^{ns} is the observed, nonspecific binding constant of endo III to high molecular weight DNA. 19-K_{obs}^{ns} is the observed, nonspecific binding constant of endo III to undamaged duplex 19-mer. 19-K_{obs}^{sp} is the observed, specific binding constant of endo III to a duplex 19-mer having a central AP or rAP site. K_2 is the ratio (HM-K_{obs}^{ns})/(19-K_{obs}^{sp}).

0006-2960/95/0434-2537$09.00/0

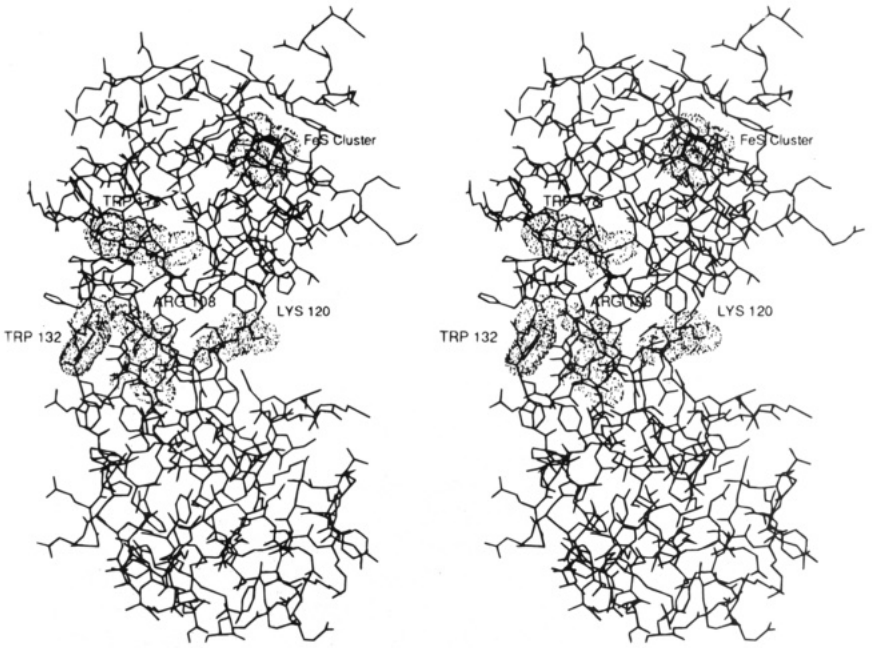

FIGURE 1: Structure of endo III showing explicit location of Trp^{132}, somewhat exposed in the helix−turn−helix region that contains the Lys^{120} active site for Schiff base formation, and Trp^{178}, more embedded in the protein near the Fe-S center. van der Waals radii of side chain atoms of Trp^{132}, Arg^{108}, Lys^{120}, Trp^{178}, and the Fe-S center are indicated to show their proximity to each other.

companying paper we characterize binding by methods of gel retardation and footprinting. Detailed investigation of the catalytic site is underway by mutagenesis and chemical trapping.

The intrinsic tryptophan fluorescence comes from the only two tryptophan residues of endo III, Trp^{132} and Trp^{178}, whose locations are shown in Figure 1 as they are found in the overall crystal structure of endo III (Kuo et al., 1992). Endo III contains two major domains: a six-helix domain (residues 22−132), which contains the Lys^{120} active site for Schiff base formation during AP lyase activity, and a four-helix domain (residues 1−21 and 133−211) containing a 4Fe-4S cluster. Trp^{132} is in the cleft between the two domains and so may be sensitive to conformational change brought on by substrate binding. Trp-178 is buried in the general vicinity of the 4Fe−4S group at one end of the endo III molecule.

Fluorescence lifetimes of tryptophan are highly sensitive to accessibility of quenchers. If tryptophan is accessible to anions, iodide provides a source of collisional quenching (Lakowicz, 1983; Lehrer, 1971; Maegley et al., 1992). One explanation for DNA-induced quenching is that excitation transfer from tryptophan to nearby bases of DNA occurs when the separation of tryptophan and bases is in the 5−10 Å range; the closer the distance, the more effective the quenching (Härd et al., 1989). Proximity of a tryptophan to a charged protein group (such as Arg^{108} here) can also lead to fluorescence quenching (Lakowicz, 1983). Thus, many DNA-binding proteins show quenching of their tryptophan fluorescence when DNA is bound. Fluorescence quenching has been used both to monitor general nonspecific binding of protein to single-strand and duplex oligonucleotides (Kelly & von Hippel, 1976; Kelly et al., 1976; Pörschke & Rush, 1983) and to monitor potentially stronger binding to a specific oligonucleotide site (Kowalczykowski et al., 1981; Maegley et al., 1992). Quenching of tryptophan in a model Lys-Trp-Lys peptide has been attributed to tryptophan intercalation into AP sites in damaged DNA (Behmoraras et al., 1981). Binding of protein to DNA need not always lead to tryptophan fluorescence quenching; there is a 40% increase in fluorescence when *Eco*RI DNA methyltransferase binds to a 14-mer recognition site (Maegley et al., 1992).

MATERIALS AND METHODS

Endonuclease III. Endo III from *E. coli* was purified to homogeneity and tested for *N*-glycosylase and AP lyase activity as described previously (Asahara et al., 1989). Protein concentration was determined from absorbance at 280 nm (extinction coefficient $\epsilon_{280} = 31.5\ cm^{-1}\ mM^{-1}$) by the method of Gill and von Hippel (1989).[2] Stock solutions of protein at 30 μM were kept in 50% glycerol, 50 mM potassium phosphate buffer, pH 6.8, and diluted to 0.8 μM protein by addition of 50 mM potassium phosphate buffer containing 100 mM KCl just before the experiment. A solution containing 100 mM KCl was used during the fluorescence experiments because activity assays, gel shifts, and footprinting studies were all done with this concentration of KCl.

High Molecular Weight DNA Substrates. Duplex poly(dAdT) and single-stranded poly(dT) were purchased from Pharmacia. Salmon sperm DNA was purchased from Sigma and purified according to the phenol extraction methods of Sambrook et al. (1989). To create random AP sites in poly(dAdT), acid/heat depurination at pH 5 and 70°C was performed. [See Figure 2 of Lindahl and Nyberg (1972) which indicates a reaction rate of 3.8×10^{-7} base pairs/s for production of depurinated ethanol-soluble material from

[2] According to the method of Gill and von Hippel (1989), the optical density from the denatured protein in 6 M Gdn·HCl was determined at 280 nm. This optical density was then related to the absorbance of the tyrosine, tryptophan, and cysteines whose concentrations can be calculated from the sequence-determined amino acid composition (Asahara et al., 1989) and from tables provided by Gill and von Hippel (1989). The optical density of the denatured protein was then referred to the optical density of the native protein, and the extinction coefficient of native protein was determined.

poly(dAdT).] In a 24 h reaction time we estimate that one depurinated AP site per 30 base pairs was created. Such a method of creating AP sites is considerably less quantitative and less explicit in its location than the very specific methods described below for creating a central AP site in a well-defined oligonucleotide. AP poly(dAdT) provided by the acid/heat depurination method was only used to discover a qualitative fluorescence difference between how endo III binds to intact high molecular weight duplex DNA and how endo III binds to AP-containing high molecular weight duplex DNA.

Synthesis of Oligonucleotide Substrates. Oligonucleotide 19-mers d(GCAGCGCAG(U)CAGCCGACG) and d(CGTCG-GCTGACTGCGCTGC) were synthesized on an Applied Biosystems Model 381A DNA synthesizer and purified by HPLC (Fu et al., 1992; O'Handley et al., 1995). d-(GCAGCGCAG(U)CAGCCGACG) was incubated with uracil-DNA glycosylase from *E. coli* to produce an apyrimidinic site in the center of the oligomer. The resulting oligomer d(GCAGCGCAG(AP)CAGCCGACG) was in turn reduced with sodium borohydride to create a reduced AP site, d(GCAGCGCAG(rAP)CAGCCGACG), at the center of the oligomer. The concentrations of unmodified oligomers were determined by using ϵ_{260} values calculated from published data (Fasman, 1975), as indicated in Fu et al. (1992), the single-stranded 19-mers that contained a central uracil, a central AP site, or a central reduced AP site were annealed to the complementary A-containing 19-mer to provide duplex (U•A)-19-mers, (AP•A)-19-mers, and (rAP•A)-19-mers, respectively. (rAP•A)-19-mer was used in these binding studies to provide a site similar to an AP site which could not be cleaved by endo III. Melting studies on a 13-mer indicated that these 13-mer forms were duplex at room temperature down to $\sim 10^{-8}$ M; 19-mers were chosen for this present study because we expected them to be even more stable. Because of higher yield, ease of purification, and overall need for larger amounts of oligonucleotide for these fluorescence studies than for gel retardation and footprinting studies, the 19-mer was the oligonucleotide chosen for these fluorescence studies. Because higher molecular weight 25-mer and 39-mer oligonucleotides ultimately became the molecules of choice for the accompanying retardation and footprinting studies (O'Handley et al., 1995), comparative fluorescence quenching experiments at low concentrations of oligonucleotide and enzyme were done with (rAP•A)-39-mer and (U•A)-39-mer.

Fluorescence Measurements. The fluorescence experiments were performed either on a Perkin Elmer LS 50 luminescence spectrometer or on an RF 2500 fluorescence spectrometer. A Fotodyne buffer cooler circulator was used to control the temperature at 21.0 °C. An excitation wavelength of 290 nm, slit width 5 nm, and an emission wavelength of 347 nm, slit width 5 nm, were applied. The fluorescence intensity was corrected for the inner filter effect resulting from absorbance of DNA. At 290 nm the extinction coefficient per base pair from poly(dAdT) was 1.7 mM^{-1} cm^{-1}, and for the duplex 19-mer the extinction coefficient per base pair was 3.3 mM^{-1} cm^{-1} at 290 nm. An inner filter correction factor (Pörschke & Rauh, 1983), f, was applied

$$f = [2.303\epsilon c(d_2 - d_1)]/(10^{-\epsilon c d_1} - 10^{-\epsilon c d_2}) \approx 10^{A/2} \quad (1)$$

where ϵ is the extinction coefficient per base pair of DNA at 290 nm, c is the concentration of DNA in base pairs, d_2 and d_1 define the length within the fluorescence cuvette from which fluorescence is collected, and A ($= \epsilon c$) is the absorbance of the DNA at the exciting wavelength of 290 nm. By taping off sections of the fluorescence cuvette, we determined that d_2 and d_1 were respectively 0.6 and 0.4 cm. The corrected fluorescence intensity F in the presence of DNA having absorbance A at 290 nm was $F = fF_u$, where F_u is the uncorrected fluorescence intensity.

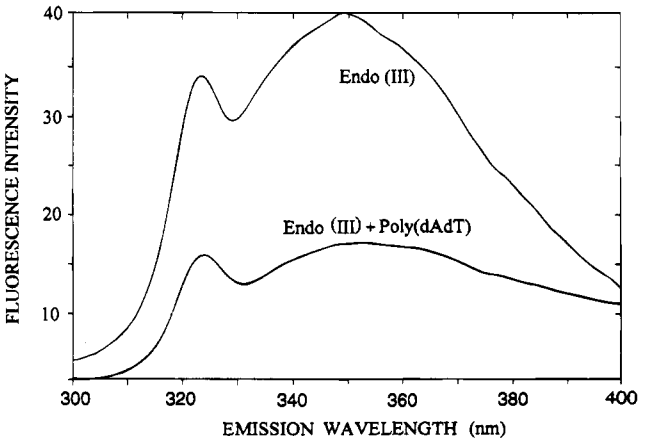

FIGURE 2: Fluorescence emission spectra of endo III and endo III plus poly(dAdT). The solvent was 50 mM potassium phosphate, pH 6.8, 100 mM KCl, the endo III concentration was 0.8 μM, and the poly(dAdT) concentration was 36 μM. (The inner filter correction was 1.06.) The peak at approximately 325 nm is the water Raman scattering peak.

In the course of a titration with a particular type of DNA, successive aliquots of the DNA were added to the binding mixture and gently agitated. The fluorescence intensity was measured following each addition, and the unquenched fluorescence was immediately obtained from endo III to which the same volume of buffer had been added. Following an inner filter correction, the fluorescence was calculated as a percentage of unquenched fluorescence, i.e., the quantity F/F_o was calculated and expressed as a percent. F/F_o was plotted vs concentration of added DNA.

RESULTS

Fluorescence Spectra. Fluorescence spectra obtained with an excitation wavelength of 290 nm are shown in Figure 2. The emission maximum from the enzyme in absence of quenchers occurs at 348 ± 2 nm, and the width at half-height is approximately 65 nm. The partially quenched spectrum in the presence of high molecular weight polynucleotide poly(dAdT) in the ratio of 36 base pairs per endo III is shown.

Accessibility of the Tryptophans in Endo III to Iodide Quencher. Quenching by iodide of tryptophan fluorescence was followed with addition of successive aliquots of 5 M KI. A comparable concentration of NaCl applied to DNA-free endo III led to negligible quenching. Quenching of two populations of fluorophores, one of which is more accessible to quencher, can be analyzed by a modified form of the Stern−Volmer equation to determine the accessible fraction, f_a, where K_Q is the collisional constant of the accessible fraction [Lehrer, 1971; Lakowicz, 1983 (pp 279−284)]:

$$F_o/(F_o - F) = 1/(f_a[I^-]K_Q) + 1/(f_a) \quad (2)$$

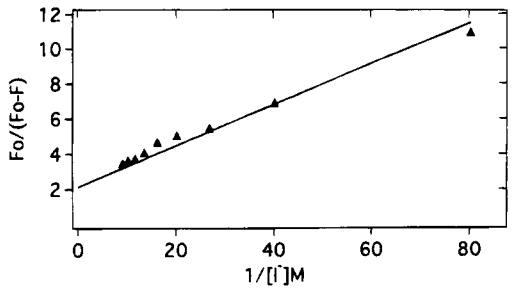

FIGURE 3: Modified Stern–Volmer plot showing evidence for two different types of fluorophores with different accessibility to iodide. The fraction of nonaccessible sites is 0.47 ± 0.10.

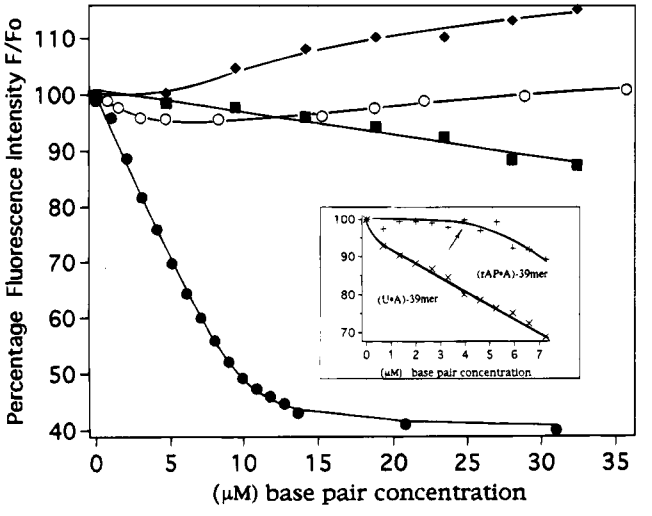

FIGURE 4: Titration of endo IIIs tryptophan fluorescence vs poly(dAdT) (●), poly(dT) (○), (U•A)-19-mer (■), and (rAP•A)-19-mer (◆). Concentration of endo III was 0.8 μM for titrations with poly(dAdT), (U•A)-19-mer, and (rAP•A)-19-mer and 1.6 μM for titration with poly(dT). For the titration vs poly(dAdT), endo III was titrated vs duplex poly(dAdT) whose concentration was measured in base pairs; the resultant solid-line titration curve for addition of poly(dAdT) is a least-squares-fitted curve to a second order equilibrium expression (Appendix A) that has an apparent association constant of HM-K_{obs}^{ns} = 4 ± 1 × 10^7 M^{-1} and 12.2 ± 0.2 base pairs per binding site. Titrations vs poly(dT), undamaged (U•A)-19-mer, (AP•A)-19-mer, or (rAP•A)-19-mer showed much smaller change in fluorescence. The points for the poly(dT) and (rAP•A)-19-mer titrations were simply connected with no underlying theoretical significance. The linear fit to the titration data for (U•A)-19-mer is outlined in Appendix B. The inset to Figure 4 compares the fluorescence quenching from endo III at 0.1 μM concentration as brought on by (rAP•A)-39-mer (+) and (U•A)-39-mer (×). The arrow denotes the point at which the mole ratio of endo III to (rAP•A)-39-mer became 1:1.

A plot of the iodide quenching data to a modified Stern–Volmer equation is given in Figure 3, and such a plot yielded the more highly iodide-accessible fraction (f_a) of 0.47 ± 0.10.

Tryptophan Fluorescence Quenching by High Molecular Weight Polynucleotide. As shown in Figure 4 where the endo III concentration was 0.8 μM, the fluorescence decreased to a minimum of 40% of its unquenched value (i.e., there was 60% quenching) when the ratio of poly(dAdT) base pairs to endo III was greater than ~12. In the presence of a comparable concentration of single-stranded poly(dT), there was no more than 5% fluorescence quenching. The fluorescence quenching as titrated on a base pair basis due to salmon sperm DNA was superimposable with that of poly(dAdT), and the fluorescence quenching due to poly(dIdC) was very similar. Once the maximum quenching and concomitant fluorescence minimum had been reached, aliquots of 5.0 M NaCl were added, and an NaCl concentration ≥ 200 mM reversed the fluorescence quenching due to high molecular weight duplex polynucleotide.

The tryptophan fluorescence intensity in the presence of an acid-depurinated poly(dAdT) that provided ~two AP sites per endo III molecule was significantly larger (i.e., outside the range of the ~1% experimental error in the fluorescence measurements) than the fluorescence in the presence of an equal base pair concentration of intact, high molecular weight poly(dAdT). A set of bar graphs comparing the tryptophan fluorescence quenching from such heat/acid-depurinated poly(dAdT) is given in the supplementary material. This measurement on acid-depurinated poly(dAdT) was carried out prior to development of oligonucleotides with well-defined central AP sites.

Tryptophan Fluorescence in the Presence of Synthesized Oligonucleotides. Fluorescence titrations also shown in Figure 4 were carried out versus the intact duplex (U•A)-19-mer and versus the (rAP•A)-19-mer. Figure 4 indicates a small decrease in fluorescence brought on by the (U•A)-19-mer and a small increase in fluorescence brought on by the (rAP•A)-19-mer. The fluorescence change brought on by either type of 19-mer is much less than the fluorescence decrease brought on by high molecular weight DNA. Fluorescence changes brought on by simple addition of either (U•A)-19-mer or (rAP•A)-19-mer to endo III were much smaller than those brought on by poly(dAdT) even when a 1.7 mole excess of such 19-mers was added (1.7 μM of 19-mer = 32 μM base pairs.) Further resolution of such small changes is limited by inner filter effects; with a 19-mer concentration of 1.7 μM, the inner filter correction was approximately 1.13, and the resultant 13% correction was comparable with the actual fluorescence changes brought on by these 19-mers. As shown in the inset to Figure 4, the control experiments that compared fluorescence quenching brought on by (rAP•A)-39-mer versus (U•A)-39-mer verified that the damaged (rAP•A)-39-mer caused markedly less fluorescence quenching than the undamaged (U•A)-39-mer. After one (rAP•A)-39-mer per endo III had been added, there was evidnece for an increased fluorescence quenching (i.e., an increase in slope starting at the point shown by an arrow) when more (rAP•A)-39-mer was added.

Competition for Endo III between Poly(dAdT) and Oligonucleotide 19-mers As Monitored by Tryptophan Fluorescence. The fluorescence of endo III was initially titrated with poly(dAdT) in the absence of 19-mer until this fluorescence had diminished to its minimal ~40% value as shown on the left hand side of Figure 5. Duplex 19-mers were then added, as shown on the right hand side of Figure 5. The (rAP•A)-19-mer caused the fluorescence to revert to ~90% of its unquenched value, and the (AP•A)-19-mer (which could in principle provide a *catalyzable* substrate) also caused the fluorescence to revert to slightly greater than its unquenched (100%) value. Very little reversal of quenching was observed in the presence of the intact (U•A)-19-mer.

DISCUSSION

The Two Tryptophans of Endo III Are Differently Accessible to Iodide Quencher. Because the wavelength of the tryptophan fluorescence emission maximum is sensitive to

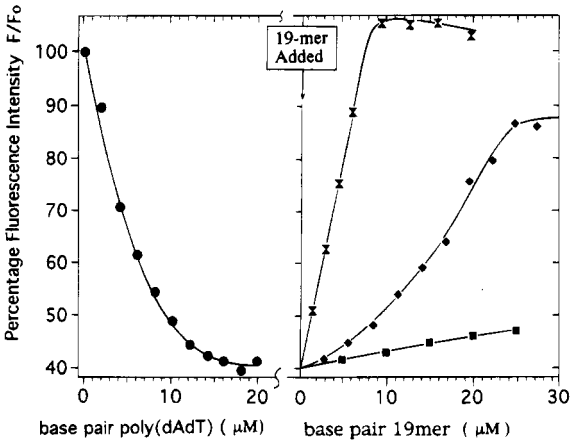

FIGURE 5: Competition experiment between poly(dAdT) and 19-mers for binding to endo III to show reversal of fluorescence quenching by (rAP•A)-19-mer (◆) and (AP•A)-19-mer (solid hourglass) but not by undamaged (U•A)-19-mer (■). The left hand part of the curve is fluorescence quenching by poly(dAdT) (●) up to a concentration of 20 μM base pairs. The right hand curves show significant reversal of the tryptophan fluorescence brought on by competition with (rAP•A)-19-mer and (AP•A)-19-mer but not by undamaged (U•A)-19-mer. (Addition of (rAP•A)-19-mer beyond 30 μM base pairs indicated that the fluorescence reached the plateau shown at slightly less than 90%.) Points in these curves were simply connected with no theoretical fitted significance.

the polarity of the tryptophan environment (Lakowicz, 1983), a wavelength maximum of >347 nm and the 65 nm width indicate a polar environment for the tryptophan(s) that contribute to the fluorescence (Burstein et al., 1973). The iodide quenching experiments and modified Stern−Volmer plot implied a different accessibility of fluorescing tryptophan(s) to anionic iodide so that about half of the tryptophans (since $f_a \sim 1/2$) are more accessible to iodide than the other half. The X-ray crystallographic data (Kuo et al., 1992) show that Trp^{132} has a 68 Å^2 solvent accessible surface compared to 18 Å^2 for Trp^{178}. The maximum possible tryptophan side chain solvent accessibility is 221 Å^2 (Hamaguchi, 1992). We conclude that the iodide quenching is consistent with two tryptophans having different solvent and anion accessibilities, where Trp^{132} is more likely to be the accessible tryptophan.

Tryptophan Fluorescence Quenching Shows Endo III Binds Nonspecifically with Poly(dAdT). Interaction of endo III with poly(dAdT) led to a quenching of about 60% of the tryptophan fluorescence. To account for the 60% quenching by long duplex DNA, it may be that one tryptophan may be highly quenched when DNA binds while the other tryptophan is only slightly quenched. Such an explanation would be consistent with Trp^{132} which is in a flexible helix−hairpin−helix region (Figure 1) as the DNA base-accessible tryptophan and Trp^{178} as the less accessible tryptophan.

Binding of duplex undamaged DNA is *nonspecific* binding since the fluorescence quenching due to it was approximately the same for poly(dAdT), salmon sperm DNA, and poly(dIdC), all duplex undamaged forms. The fluorescence quenching occurs for nonspecific binding to high molecular weight duplex DNA but *not* to single-stranded DNA. Since the fluorescence quenching from long duplex DNA diminished as the NaCl concentration increased to 200 mM, the implication is that there is a pronounced ionic character to the nonspecific binding, as has been observed with nonspecific DNA binding that is shown by repressor proteins (Jensen & von Hippel, 1976; Revzin & von Hippel, 1977). Initial nonspecific binding of the repressor protein to DNA is followed by rapid one-dimensional diffusional sliding along the DNA so that the time to locate its specific promoter sequence is decreased (Winter et al., 1981; Jack et al., 1982; Berg & von Hippel, 1985). There is then the question of whether nonspecific binding of endo III to DNA followed by a one-dimensional search for a specific damaged site, as opposed to direct three-dimensional diffusion to the damaged site, is likewise important for the catalytic mechanism of endo III. This question could be answered in future kinetic experiments from the dependence of k_{cat} and K_m upon the overall length of the damaged DNA.

From the titration curve of endo III with poly(dAdT), the number of base pairs per binding site was estimated and an apparent nonspecific binding constant inferred. Nearly stoichiometric binding up to ~12 base pairs per endo III indicated a binding constant greater than the inverse of the total endo III concentration (i.e., $>10^6$ M^{-1}) to a site having approximately 12 base pairs per bound endo III. Curvature in Figure 4 at those points where nearly 12 base pairs of poly(dAdT) per endo III were bound gave qualitative evidence that this nonspecific binding constant was large but finite. We conceived of this nonspecific binding as phenomenologically reporting the following equilibrium:

$$\text{endo III}_{\text{free}} + \text{poly(dAdT)}_{\text{free}} \overset{\text{HM-}K_{\text{obs}}{}^{\text{ns}}}{\rightleftharpoons} \text{endo III−poly(dAdT) complex} \quad (3)$$

The overall titration curve was fit to a second-order equilibrium (Appendix A) where HM-$K_{obs}{}^{ns}$ is the apparent second-order binding constant. The resultant fitted binding constant was $4 \pm 1 \times 10^7$ M^{-1}, maximum quenching was (60 ± 2)%, and the number of base pairs per bound endo III was 12.2 ± 0.2. A 12-base pair binding site would imply a nonspecific binding length of order 40 Å, comparable with the 60 × 30 × 35 Å^3 dimensions of endo III. [See the suggested endo III−DNA binding configuration in Figure 5B of Kuo et al. (1992).] We report the binding constants of endo III here in terms of the concentration of endo III as a monomer. Although free endo III is not a dimer at the micromolar concentrations used (Asahara et al., 1989), the exact composition of the DNA-binding form of endo III is not known. If endo III bound nonspecifically as a dimer, the binding site would be 24 base pairs long.

Fluorescence Quenching from 19-mer and 39-mer Oligonucleotides. The small fluorescence change due to 19-mer and 39-mer oligonucleotides *containing a central rAP* site was surprising because we knew from gel shift assays and footprinting (O'Handley et al., 1995) that there was definite endo III binding of such substrate-like molecules with a binding constant $\gg 10^6$ M^{-1}. *Specific binding of endo III to an AP site was occurring in a mode that had different fluorescence quenching than did the mode for nonspecific binding.* We noted that at the point where one endo III has been added per one (rAP•A)-39-mer (arrow in inset to Figure 4), there was an apparent change in slope of the fluorescence quenching curve; the implication was that once the central rAP site had been specifically bound the (rAP•A)-39-mer might be long enough still to have remaining, adjacent nonspecific binding sites.

The change brought on by *undamaged* (U•A)-19-mer was in the direction of decreasing fluorescence expected from

nonspecific binding, but on a base pair basis or even on a one oligonucleotide to one endo III basis, the changes were much smaller than those brought on by poly(dAdT). We wanted an estimate for the specific binding constant for binding to the (U•A)-19-mer, and so we considered the following equilibrium:

$$\text{endo III}_{\text{free}} + \text{(U•A)-19-mer}_{\text{free}} \overset{19\text{-}K_{\text{obs}}{}^{\text{ns}}}{\rightleftharpoons} \text{endo III}-\text{(U•A)-19-mer complex} \quad (4)$$

where 19-$K_{\text{obs}}{}^{\text{ns}}$ is the nonspecific binding constant for (U•A)-19-mer. From the linear decrease of fluorescence in the presence of (U•A)-19-mer, we estimated a nonspecific binding constant of order 10^5 M^{-1}. (See Appendix B.) Because competition gel shift assays have indicated that the nonspecific binding constant increases from $(4.5-32) \times 10^3$ M^{-1} for an undamaged 13-mer (O'Handley et al., 1995) to $(1-5) \times 10^5$ M^{-1} for an undamaged 39-mer (Kuo et al., 1992), there is evidence that longer oligonucleotides have higher nonspecific binding for endo III. A 19-mer would contiguously accommodate few (probably, ≤ 2) endo III molecules. The fluorescence quenching due to the (U•A)-39-mer with its larger slope implied a larger nonspecific binding constant for the (U•A)-39-mer than for the (U•A)-19-mer. The nonspecific binding of the (U•A)-39-mer could be stronger than to the (U•A)-19-mer since there will be a larger number of nonspecific binding sites on a (U•A)-39-mer than on a (U•A)-19-mer or since there is a greater potential for cooperative, contiguous nonspecific binding of several endo III molecules on the longer (U•A)-39-mer. High molecular weight duplex DNA would contiguously accommodate many more endo III molecules than either of these short oligonucleotides. (See Appendix C for discussion of possible cooperative aspects of nonspecific binding of endo III to high molecular weight DNA.)

Specific Binding to the AP Site. Initial findings led us to believe that binding of endo III to an AP site was qualitatively different from nonspecific binding to intact duplex DNA. First, the fluorescence quenching of endo III that had bound to high molecular weight DNA containing heat/acid-depurinated AP sites was less than the quenching brought on by the same DNA in undamaged form. Second, the fluorescence quenching by (rAP•A)-19-mer and (rAP•A)-39-mer was small even though there was evidence from gel retardation and footprinting that endo III would significantly bind even a (rAP•A)-13-mer at submicromolar concentrations. The mode in which endo III was specifically binding to AP or rAP centers was not being directly reported by fluorescence quenching.

Our competition studies in the presence of damaged (rAP•A)-19-mer and (AP•A)-19-mer showed a clear diminishment of the fluorescence quenching initially brought on by nonspecific binding to poly(dAdT), and from the diminishment a specific binding constant could be inferred. To interpret the diminishment in fluorescence brought on by (rAP•A)-19-mer, we considered the two following competitive equilibria between endo III as it bound nonspecifically to poly(dAdT) with apparent binding constant HM-$K_{\text{obs}}{}^{\text{ns}}$ and endo III as it bound specifically to (rAP•A)-19-mer with specific binding constant 19-$K_{\text{obs}}{}^{\text{sp}}$:

$$\text{endo III}_{\text{free}} + \text{poly(dAdT)}_{\text{free}} \overset{\text{HM-}K_{\text{obs}}{}^{\text{ns}}}{\rightleftharpoons} \text{endo III}-\text{poly(dAdT) complex} \quad (5)$$

$$\text{endo III}_{\text{free}} + \text{(rAP•A)-19-mer}_{\text{free}} \overset{19\text{-}K_{\text{obs}}{}^{\text{sp}}}{\rightleftharpoons} \text{endo III}-\text{(rAP•A)-19-mer complex} \quad (6)$$

The net result of these two competitive equilibria was

$$\text{endo III}-\text{(rAP•A)-19-mer complex} + \text{poly(dAdT)}_{\text{free}} \overset{K_2}{\rightleftharpoons} \text{endo III}-\text{poly(dAdT) complex} + \text{(rAP•A)-19-mer}_{\text{free}} \quad (7)$$

where $K_2 = (\text{HM-}K_{\text{obs}}{}^{\text{ns}})/(19\text{-}K_{\text{obs}}{}^{\text{sp}})$. We estimated from the fluorescence recovery brought on by (rAP•A)-19-mer in Figure 5 a value of $K_2 = 1.05 \pm 0.5$ (see Appendix D). This value of K_2 translated into a specific binding constant for the (rAP•A)-19-mer of 4×10^7 M^{-1}, a number somewhat larger that the binding constant of (rAP•A)-13-mer which gel shift assays determined to be in the range (2×10^6)-(2×10^7) M^{-1} (O'Handley et al., 1995). (The reader should note that these numbers are specific binding constants for the (rAP•A)-19-mer or (rAP•A)-13-mer, *not* kinetic association constants.) A question may arise whether endo III specifically bound to an rAP site may simultaneously be nonspecifically bound to duplex DNA but in such a conformation that tryptophan fluorescence is lost. That question cannot be easily answered by these fluorescence measurements. However, gel competition assays have shown a physical competition for endo III between high molecular weight duplex poly(dIdC) and (rAP•A)-19-mer such that endo III is not simultaneously bound to both long duplex DNA and short (rAP•A)-19-mer (O'Handley, S., and Cunningham, R. P. Unpublished communication).

Although (AP•A)-19-mer was expected to be a catalyzable substrate, we were surprised that addition of this AP oligonucleotide also led to recovery of fluorescence in competition with poly(dAdT) as shown in Figure 5. The fluorescence recovery brought on by (AP•A)-19-mer persisted as if the (AP•A)-19-mer, or conceivably a catalyzed product of it, remained bound to the endo III. The recovery was sufficiently abrupt and apparently stoichiometric with concentration of added (AP•A)-19-mer that we can only infer that the binding constant for the (AP•A)-19-mer (or conceivably a product of it which binds to endo III) was at least 1 order of magnitude larger than 4×10^7 M^{-1} (see Appendix D).

Structural Inferences. There must be a structural basis for the difference in fluorescence quenching as brought on by nonspecific binding of endo III to undamaged poly(dAdT) versus specific binding to AP or rAP substrate. Arg^{108} and Trp^{132} shown in Figure 1 are at opposite extremes of the cleft-centered sequence about the Lys^{120} active site. Yet the ϵ and ζ indole ring carbons of Trp^{132} are within 4.5 Å of guanidinium nitrogens of Arg^{108}. To account for loss of fluorescence upon specific binding, we suggest that the helix−hairpin−helix cleft centered on Lys^{120} alters its conformation on binding an AP or rAP site so as to remove Trp^{132} from proximity to DNA bases and possibly from proximity to the charged Arg^{108} side chain. It follows that endo III should be positioned differently for specific binding to an AP site versus nonspecific binding to undamaged DNA.

In analogy with the suggested conformational differences between nonspecific, electrostatically bound *lac* repressor and specific hydrogen-bonded *lac* repressor [Winter et al., 1981 (p 6975)], endo III may have a different conformation for its two types of binding. This difference in position, and conceivably conformation, would correlate with the difference between the five- to seven-base pair size of the specific, AP-centered binding site determined by footprinting (O'Handley et al., 1995) versus the 12-base pair size of the nonspecific binding site determined from fluorescence measurements.

ACKNOWLEDGMENT

We thank Prof. Jacquelyn Fetrow, Department of Biological Sciences, SUNY at Albany, for providing Figure 1 and measuring interatomic distances.

SUPPLEMENTARY MATERIAL AVAILABLE

Set of bar graphs comparing the fluorescence quenching from 1.6 μM endo III in the presence of undamaged poly(dAdT) and in the presence of heat/acid-depurinated poly(dAdT) in which there were an estimated two damaged bases per enzyme (2 pages). Ordering information is given on any current masthead page.

APPENDICES

These appendices explain details of how fluorescence quenching was related to binding equilibria.

APPENDIX A

Nonspecific Binding of Endo III to Long, Undamaged Duplex DNA. In explaining the nonspecific binding of endo III to long, undamaged duplex DNA, notably poly(dAdT), we considered the apparent equilibrium between free and complexed ("bound") sites on the DNA according to the straightforward method of Woodbury and von Hippel (1983) (p 4734, footnote 1). We use this method under "stoichiometric" binding conditions for endo III binding to a DNA lattice that is nearly occupied by contiguously bound endo III molecules to obtain the apparent binding constant (HM-K_{obs}^{ns}) for endo III to high molecular weight duplex DNA and the number (n) of base pairs per binding site. Thus in the terminology of Woodbury and Von Hippel (1983):

$$S_F + P \overset{\text{HM-}K_{obs}^{ns}}{\rightleftharpoons} S_B$$

S_F = concentration of free DNA binding sites for endo III, S_B = concentration of bound endo III on DNA; and P = free protein concentration.

We related the fluorescence which remains in the presence of DNA to the fraction of endo III would is bound to DNA as follows:

$$F/F_o = 100 - \Delta F \cdot f_b$$

where f_b = fraction of endo III bound to DNA, F/F_o = percentage of initial tryptophan fluorescence remaining after a fraction, f_b, of endo III is bound to DNA, and ΔF = maximum percent quenching when all endo III is bound.

$$f_b = [1/(2P_T)]\cdot[D/n + 1/(\text{HM-}K_{obs}^{ns}) + P_T - [(D/n + 1/(\text{HM-}K_{obs}^{ns}) + P_T)^2 - 4(D/n)P_T]^{1/2}]$$

where P_T = total enzyme concentration, D = total concentration of DNA in base pairs, and D/n = total concentration of contiguous endo III binding sites.

APPENDIX B

Estimate of the Weak Binding Constant to (U·A)-19-mer. When there was small fluorescence quenching and weak, nonspecific binding of endo III to undamaged (U·A)-19-mer, we used the following procedure to estimate the apparent nonspecific second-order binding constant, 19-K_{obs}^{ns}, for the binding of endo III to (U·A)-19-mer. As a function of added (U·A)-19-mer, the initial slope of the fluorescence change can be related to this apparent binding constant. If [UA] is the concentration of (U·A)-19-mer (in micromolar of 19-mer, not base pairs), F/F_o is the percentage of initial tryptophan fluorescence remaining after a fraction, f_b, of endo III is bound to (U·A)-19-mer, ΔF is the maximum percent quenching, and P_t = total enzyme present, then the initial slope is

$$d(F/F_o)/d[UA] = -\Delta F(19\text{-}K_{obs}^{ns})/[1 + (19\text{-}K_{obs}^{ns})P_t]$$

This slope was (-9.7 ± 1.0)% per micromolar (U·A)-19-mer. We can estimate 19-K_{obs}^{ns} if we have a value for ΔF. Because the amount of (U·A)-19-mer needed to saturate endo III leads to an overwhelming inner filter correction and prevents us from experimentally measuring ΔF, we have assumed ΔF to be 60% as is the case with binding of poly(dAdT). We then calculated that 19-$K_{obs}^{ns} = 1.4 \times 10^5$ M^{-1}. Because of the uncertainty in ΔF, we expect 19-K_{obs}^{ns} to be of the order 10^5 M^{-1}. The slope of fluorescence quenching, $d(F/F_o)/d[UA]$, for the (U·A)-39-mer quenching was 1 order of magnitude larger than for the (U·A)-19-mer, whence the predicted value of 39-K_{obs}^{ns} would be of order 10^6 M^{-1}.

APPENDIX C

Cooperativity of Nonspecific Binding of Endo III to Long, Undamaged DNA. We infer that under our experimental conditions the nonspecific binding of endo III to high molecular weight DNA has a cooperative character. The reason for our inference is that if there were not cooperativity when endo III binds high molecular weight DNA, then (1) the DNA lattice would entropically resist being saturated even at high ratios of endo III to DNA (McGhee & von Hippel, 1974) and the nearly the stoichiometric binding of poly(dAdT) would not be observed and (2) the marked difference in binding constants between (U·A)-19-mer, where few contiguous endo IIIs can bind, and long DNAs, where many contiguous endo IIIs can bind, would not be so pronounced. Such nonspecific, cooperative binding has been observed with many DNA-binding proteins and lends itself in the limit of high cooperativity to interpretation by a simple second-order equilibrium. The cooperativity may be due most straightforwardly to interactions between adjacent endo III molecules as they bind to DNA or, more subtly, to conformational change involving DNA distortion combined with protein−protein and protein−DNA interactions. *In vivo* where endo III is a rare species, such cooperative, nonspecific binding with other endo III molecules would be unlikely;

with our experiments (and with many *in vitro* binding and activity studies) where concentrations of endo III are in the micromolar regime and DNA base pair concentrations even larger, cooperative nonspecific binding may be important.

APPENDIX D

Estimating the Competitive Equilibrium Constant, K_2. The expression for K_2 is

$$K_2 = [[(\text{rAP•A})\text{-19-mer}]/[\text{poly(dAdT)}] \times [\text{endo III}-\text{poly(dAdT) complex}]/[\text{endo III}-(\text{rAP•A})\text{-19-mer complex}]]$$

The concentrations of [endo III−(rAP•A)-19-mer complex] and [endo III−poly(dAdT) complex] were determined from the magnitude of fluorescence quenching. When F_1 is the fluorescence (≈90%) from endo III fully complexed with (rAP•A)-19-mer, F_2(≈40%) is the fluorescence from endo III completely complexed with poly(dAdT), and F is the fluorescence quenching measured from endo III in the presence of both poly(dAdT) and (rAP•A)-19-mer, then the ratio [endo III−poly(dAdT) complex]/[endo III−(rAP•A)-19-mer complex] = $(F_1 - F)/(F - F_2)$. [Poly(dAdT)] is the free poly(dAdT) concentration measured in micromolar 12-base pair binding sites; [(rAP•A)-19-mer] is the concentration of free (rAP•A)-19-mer in micromolar oligonucleotides. The concentration of free (rAP•A)-19-mer was estimated from the total amount of (rAP•A)-19-mer which had been added up to the point where fluorescence was measured minus the concentration of endo III−(r-AP•A)-19-mer complex. The concentration of free poly(dAdT) was estimated from the total amount of poly(dAdT) which had been added up to the point where fluorescence was measured minus the concentration of endo III−poly(dAdT) complex. From the (rAP•A)-19-mer-induced fluorescence recovery (Figure 5) where F ranged between 40% and 88%, values of K_2 were calculated whence an average value of $K_2 = 1.05 \pm 0.5$ was obtained. It was not possible to obtain a specific estimate of the binding constant for (AP•A)-19-mer because the binding of (AP•A)-19-mer was so stoichiometric until ~100% fluorescence was reached that the concentration of free (AP•A)-19-mer was ≈0, and this led to K_2 values that were extremely small and 19-K_{obs}^{sp} values for the binding of (AP•A)-19-mer that would be large ($>10^8$ M^{-1}).

REFERENCES

Asahara, H., Wistort, P. M., Bank, J. F., Bakerian, R. H., & Cunningham, R. P. (1989) *Biochemistry 28*, 4444−4449.

Behmoaras, T., Tolumé, J.-J., & Hélène, C. (1981) *Proc. Natl. Acad. Sci. U.S.A. 78*, 926−930.

Berg, O. G., & von Hippel, P. H. (1985) *Annu. Rev. Biophys. Biophys. Chem. 14*, 131−160.

Burstein, E. A., Vedenkina, N. S., & Ivkova, M. N. (1973) *Photochem. Photobiol. 18*, 263−279.

Doetsch, P. W., & Cunningham, R. P. (1990) *Mutat. Res. 236*, 173−201.

Doetsch, P. W., Henner, W. D., Cunningham, R. P., Toney, J. H., & Helland, D. E. (1987) *Mol. Cell. Biol. 7*, 26−32.

Fasman, G. D. (1975) *CRC Handbook of Biochemistry and Molecular Biology: Nucleic Acids*, 3rd ed., Vol. I, p 589, CRC Press, Inc., Boca Raton, FL.

Fu, W., O'Handley, S., Cunningham, R. P., & Johnson, M. K. (1992) *J. Biol. Chem. 267*, 16135−16137.

Gill, S. C., & von Hippel, P. H. (1989) *Anal. Biochem. 182*, 319−326.

Hamaguchi, K. (1992) *The Protein Molecule Conformation, Stability, and Folding*, pp 74−81, Japan Scientific Societies Press, Tokyo.

Härd, T., Sayre, M. H., Geiduschek, E. P., & Kearns, D. R. (1989) *Biochemistry 28*, 2813−2819.

Jack, W. E., Terry, B. J., & Modrich, P. (1982) *Proc. Natl. Acad. Sci. U.S.A. 79*, 4010−4014.

Jensen, D. E., & von Hippel, P. H. (1976) *J. Biol. Chem. 251*, 7198−7214.

Katcher, H. L., & Wallace, S. S. (1983) *Biochemistry 22*, 4071−4081.

Kelly, R. C., & von Hippel, P. H. (1976) *J. Biol. Chem. 251*, 7229−7239.

Kelly, R. C., Jensen, D. E., & von Hippel, P. H. (1976) *J. Biol. Chem. 251*, 7240−7250.

Kowalczykowski, S. C., Lonberg, N., Newport, J. W., & von Hippel, P. H. (1981) *J. Mol. Biol. 145*, 75−104.

Kuo, C.-F., McRee, D. E., Fisher, C. L., O'Handley, S. F., Cunningham, R. P., & Tainer, J. A. (1992) *Science 258*, 434−440.

Lakowicz, J. R. (1983) *Principles of Fluorescence Spectroscopy*, pp 257−274, Plenum Press, New York.

Lehrer, S. S. (1971) *Biochemistry 10*, 3254−3263.

Lindahl, T., & Nyberg, B. (1972) *Biochemistry 11*, 3610−3618.

Maegley, K. A., Gonzalez, L., Smith, D. W., & Reich, N. O. (1992) *J. Biol. Chem. 267*, 18527−18532.

McGhee, J. D., & von Hippel, P. H. (1974) *J. Mol. Biol. 86*, 469−489.

O'Handley, S., Scholes, C. P., & Cunningham, R. P. (1995) *Biochemistry 34*, 2528−2536.

Pörschke, D., & Rush, H. (1983) *Biochemistry 22*, 4737−4745.

Revzin, A., & von Hippel, P. H. (1977) *Biochemistry 16*, 4769−4776.

Sambrook, J., Fritsch, E. F., & Mariatis, T. (1989) *Molecular Cloning, a Laboratory Manual − Second Edition*, Appendix E.3, Cold Spring Harbor Symposium Press, Cold Spring Harbor, NY.

Winter, R. B., Berg, O. G., & von Hippel, P. H. (1981) *Biochemistry 20*, 6961−6977.

Woodbury, C. P., & von Hippel, P. H. (1983) *Biochemistry 22*, 4730−4737.

BI941587V